

Cost-Aware Robust Tree Ensembles for Security Applications

Yizheng Chen, Shiqi Wang, Weifan Jiang, Asaf Cidon, and Suman Jana
Columbia University

Abstract

Features of security classifiers have various costs to be manipulated. The costs are asymmetric across features and to the directions of changes, which cannot be precisely captured by existing cost models based on L_p -norm robustness. In this paper, we utilize such domain knowledge to increase the evasion cost against security classifiers, specifically, tree ensemble models that are widely used by security tasks. We propose a new cost modeling method to capture the domain knowledge of features as constraint, and then we integrate the cost-driven constraint into the node construction process to train robust tree ensembles. During the training process, we use the constraint to find data points that are likely to be perturbed given the costs of the features, and we optimize the quality of the trees using a new robust training algorithm. Our cost-aware training method can be applied to different types of tree ensembles, including random forest model that cannot be robustly trained by previous methods. Using twitter spam detection as the security application, our evaluation results show that training cost-aware robust model can rank high cost features as the most important ones, and increase the adaptive attack cost by $6.4\times$ compared to the baseline. Our code is available at <https://github.com/surrealxyz/growtrees>.

1 Introduction

Many machine learning classifiers are deployed in security-critical settings where adversaries try to evade them almost as soon as they are deployed. Unlike perturbing features (e.g., pixels, words) in non-security related applications, manipulating security features incurs very different costs. For example, it is cheaper to purchase new domain names than to rent new hosting servers to evade a spam filter [34]. In addition, a feature may be expensive to increase, but easy to decrease. For example, it is easier to remove a signature from a malware than to add one signed by Microsoft to it [25]. We need cost modeling methods to capture such security domain knowledge, and utilize the knowledge to increase the cost of evading security classifiers.

However, existing cost modeling based on L_p -norm is not suitable for security, since it assumes uniform cost across different features and symmetric cost to increase and decrease the features. Attacks and defenses under L_p -norm are limited

at evaluating and increasing the robustness of security classifiers against realistic adversaries who are aware of such costs. Moreover, many recent works focus on improving the robustness of neural network models [17, 19, 23, 33, 35, 37, 38, 47–50], whereas security applications widely use tree ensemble models such as random forest (RF) and gradient boosted decision trees (GBDT) to detect malware [31], phishing [16, 20, 24], and online fraud [29, 39, 45], etc. Despite their popularity, the robustness of these models, especially against a strong adversary is not very thoroughly studied [11, 27, 41]. The discrete structure of tree models brings new challenges to the robustness problem. Training trees does not rely on gradient-guided optimization, but rather by enumerating potential splits to maximize the gain metric (e.g., Information gain, Gini impurity reduction, or loss reduction). Integrating additional knowledge makes the enumeration intractable.

In this paper, we propose a systematic method to train cost-aware robust tree ensemble models for security, by integrating domain knowledge of feature manipulation costs. To address the aforementioned challenges, we first propose a cost modeling method that projects the domain knowledge about features into cost-driven constraint. Then, we integrate the constraint into the training process as if an arbitrary attacker under the cost constraint is trying to maximally degrade the quality of potential splits (Equation (10) in Section 3.2.2). We propose an efficient robust training algorithm that solves the maximization problem across different gain metrics and different types of models. Notably, our robust algorithm can train random forest in scikit-learn (e.g., using entropy or Gini impurity), widely used by security applications, which cannot be robustly trained by the previous method [6, 11]. Lastly, we evaluate adaptive attack against our robust training method, as a step towards understanding robustness against realizable attacks. We propose an attack cost function as the minimization objective of the strongest whitebox attacker against tree ensembles (the Mixed Integer Linear Program attacker).

Our robust training method incorporates the cost-driven constraint into the node construction process of growing trees, as shown in Figure 1. When any potential split $x^j < \eta$ (on the j -th feature) is being considered, due to the constraint $C(j)$, there is a range of possible values a data point can be changed into for that feature (formally defined in Section 3.1.1). Thus, data points close to the splitting threshold η can potentially cross the threshold. For example, on a low cost feature, many

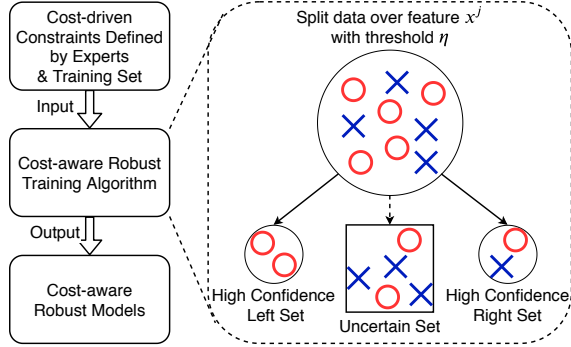


Figure 1: An overview of cost-aware robust tree ensemble training process. Our robust training algorithm incorporates the cost-driven constraint while constructing nodes. The constraint specifies the set of data points that can potentially cross the split threshold η given domain knowledge about the j -th feature, i.e. uncertain set.

data points can be easily perturbed to either the left child or the right child. Therefore, the constraint gives us a set of uncertain data points that can degrade the quality of the split, as well as data points that cannot be moved from the two children nodes. We need to quantify what is the worst quality of the split under the constraint, in order to compute the gain metric. To efficiently solve this, we propose a robust training algorithm that iteratively assigns training data points to whichever side of the split with the worse gain, regardless of the choice of the gain function and the type of tree ensemble model. As an example, we can categorize every feature into negligible, low, medium, or high cost to be increased and decreased by the attacker. Then, we use a high-dimensional box as the constraint. Essentially, the constraint gives the attacker a larger increase (decrease) budget for features that are easier to increase (decrease), and smaller budget for more costly features. The cost-driven constraint helps the model learn robustness that can maximize the cost of evasion for the attacker. This utilizes the security expert domain knowledge on features to increase the robustness of models. We have implemented our training method in state-of-art tree ensemble learning libraries: gradient boosted decision trees in xgboost [13], and random forest in scikit-learn [4].

Since none of the existing training techniques support cost modeling of features, we first evaluate the performance of our new training algorithm without the cost-driven constraint, against the state-of-the-art robust tree ensemble training method [11]. To be consistent with existing work, we follow the same settings to train a total of 20 models over 4 benchmark datasets with the goal of improving robustness against attackers bounded by L_∞ -norm (Section 4.2). In the gradient boosted decision trees evaluation, our robust training algorithm achieves on average $2.94\times$ and $1.26\times$ improvement over the baseline and state-of-the-art robust training algorithm [11] respectively, in the minimal L_∞ distance required to evade the model. In addition, we show that our al-

gorithm provides better solutions to the optimization problem than the state-of-the-art [11] in 93% of the cases on average (Section 4.2.4). For the random forest model, we are the first to provide a general robust training algorithm over arbitrary gain metrics, and therefore we evaluate against the regular training in scikit-learn. On average over the four benchmarking datasets, we achieve $3.2\times$ robustness improvement in the minimal L_∞ evasion distance compared to the baseline. This shows that our core training technique alone has made significant improvements to solve the robust optimization problem.

Next, we evaluate the cost-aware robust training method for security, using twitter spam URL detection as a case study. We reimplement the feature extraction over the dataset from [32] to detect malicious URLs posted by twitter spammers. The features capture that attackers reuse hosting infrastructure resources, use long redirection chains across different geographical locations, and prefer flexibility of deploying different URLs. Based on domain knowledge, we specify the cost-driven constraint to train a robust model, with key results summarized as follows. First, while the regularly trained model ranks low cost features as most important, the cost-aware robust model ranks the most costly features as the most important ones. This shows that the cost-aware robust training can guide the model to utilize more information from high cost features. Second, our cost-aware robust model can increase the minimal attack cost for the strongest whitebox attacker [27] to evade the robust model. We optimize an adaptive attack objective (i.e., weighted sum of feature increases and decreases) according to the trained constraint, that minimizes the attack costs against the twitter spam classifier. Our results show that the adaptive attacker needs on average $6.4\times$ cost to evade our robust model compared to the baseline model.

Our contributions are summarized as the following:

- We propose a new cost modeling method to translate domain knowledge about features into cost-driven constraint. Using the constraint, we can train models to utilize domain knowledge outside the training data.
- We propose a new robust training algorithm to train cost-aware robust tree ensembles for security, by integrating the cost constraint. Our algorithm can be applied to random forest model in scikit-learn, widely used by security tasks, that cannot be robustly trained by previous works.
- We use twitter spam detection as the security application to train a cost-aware robust tree ensemble model. Our robust model ranks the high cost features as most important, which can increase the adaptive attack cost to evade the model by $6.4\times$.

2 Background and Related Work

2.1 Tree Ensembles

A decision tree model uses logical predicates to provide predictions. Each internal node holds a predicate over some feature values. The tree structure guides the prediction path from the root to a leaf node containing the predicted value.

An ensemble of trees consists of multiple decision trees, which aggregates the predictions from individual trees. Popular aggregation functions include the average (random forest) and the sum (gradient boosted decision tree) of the prediction values from each decision tree.

2.1.1 Notations

We use the following notations for the tree ensemble in this paper. The training dataset D has N data points with d features $D = \{(x_i, y_i) | i = 1, 2, \dots, N\}$ ($x_i \in \mathbb{R}^d, y \in \mathbb{R}$). Each input x_i can be written as a d -dimensional vector, $x_i = [x_i^1, x_i^2, \dots, x_i^d]$. A predicate p is in the form¹ of $x^j < \eta$, which evaluates the j -th feature x^j against the split threshold η . Specifically, for the i -th training data, the predicate checks whether $x_i^j < \eta$. If $p = \text{true}$, the decision tree guides the prediction path to the left child, otherwise to the right child. The prediction process repeats until x_i reaches a leaf. We use a function f to denote a decision tree, which gives a real-valued output for the input data point x with the true label y . For classification trees, $f(x)$ represents the predicted probability for the true label y .

The most common decision tree learning algorithms use a greedy strategy to construct the nodes from the root to the leaves, e.g., notably CART [10], ID3 [42], and C4.5 [43]. The algorithm greedily picks the best feature j^* and the best split value η^* for each node, which partitions the data points that reach the current node (I) to the left child (I_L) and the right child (I_R), i.e., $I = I_L \cup I_R$. The training algorithm optimizes the following objective using some score to maximize the *gain* of the split:

$$j^*, \eta^* = \arg \max_{j, \eta} \text{Gain}(I_L, I_R) = \arg \max_{j, \eta} (s(I) - s(I_L, I_R)) \quad (1)$$

In Equation (1), s denotes a scoring function. For example, we can use Shannon entropy, Gini impurity, or any general loss function to evaluate the gain. After the split, the score becomes $s(I_L, I_R)$, which can be calculated as the weighted sum of the children scores. For example, using the Gini impurity, we have $\text{Gain}(I_L, I_R) = \text{Gini}(I) - \text{Gini}(I_L, I_R)$. A common strategy to solve Equation (1) is to enumerate all the features with all the possible split points to find the maximum gain. When the dataset becomes too large to compute efficiently, different optimization methods have been proposed to approximate Equation (1), e.g., weighted quantile sketch [13]. The

¹Oblique trees which use multiple feature values in a predicate is rarely used in an ensemble due to high construction costs [40].

learning algorithm chooses the best feature split with the maximum gain, and then recursively constructs the children nodes in the same way, until the score does not improve or some pre-determined threshold (e.g., maximum depth) is reached.

A tree ensemble uses the weighted sum of prediction values from K decision trees, where K is a parameter specified by the user. Each decision tree can be represented as a function f_t . Then, the ensemble predicts the output \hat{y} as follows.

$$\hat{y} = \phi(x) = a * \sum_{t=1}^K f_t(x) \quad (2)$$

Ensemble methods use bagging [7] or boosting [21, 22, 46] to grow the decision trees. The methods avoid overfitting and improves the performance of the tree ensemble over any single decision tree. Random forest and gradient boosted decision tree (GBDT) are the most widely used tree ensembles in the industry. The random forest model uses $a = \frac{1}{K}$, and the GBDT model set $a = 1$. They use different ensemble methods to grow trees in parallel or sequentially, which we describe next.

2.1.2 Random Forest

Bagging. A random forest model uses bagging [7] to grow the trees in parallel. Bagging, i.e., bootstrap aggregation, uses a random subset of the training data and a random subset of features to train individual learners.

For each decision tree f_t , we first randomly sample N' data points from D to obtain the training dataset $D_t = \{(x_i, y_i)\}$, where $|D_t| = N'$ and $N' \leq N$. The training data sample D_t for each decision tree can be drawn with or without replacement, depending on the implementation. In the case that $N' = N$, the data points are sampled with replacement. Then, at every step of the training algorithm that solves Equation (1), we randomly select d' features in I to find the optimal split, where $d' \leq d$. The feature sampling is repeated until we finish growing the decision tree. The training data and feature sampling helps avoid overfitting of the trained model.

The key distinguishing factors for random forest model are the bagging method, and that the trees are trained independently from each other. The gain can be computed using any scoring function. We focus on the scikit-learn implementation of the random forest classifier since it is widely used by related work. In scikit-learn, a decision tree computes the predicted probability as the percentage of training samples for each class reaching the leaf. It takes the class with the highest predicted probability to be the predicted class. The ensemble realizes the majority vote by taking the most likely class given averaged predicted values from the trees.

Random forest model has been used for various security applications, e.g., detecting malware distribution [31], malicious autonomous system [30], social engineering [39], phishing emails [16, 20, 24], advertising resources for ad blocker [26], and online scams [29, 45], etc. Researchers use the model-level feature importance ranking (Section 2.1.4) as a common

approach to interpret the trained random forest model. In some cases, researchers have also analyzed the performance of the model (e.g., ROC curve) given different subsets of the features to reason about the predictive power of feature categories.

2.1.3 Gradient Boosted Decision Tree

Boosting. Gradient boosted decision tree (GBDT) model uses boosting [21, 22, 46] to grow the trees sequentially. Boosting iteratively train the learners, improving the new learner’s performance by focusing on data that were misclassified by existing learners. Gradient boosting generalizes the boosting method to use an arbitrarily differentiable loss function.

In this paper, we focus on the state-of-the-art GBDT training system xgboost [13]. When growing a new tree (f_t), all previous trees (f_1, f_2, \dots, f_{t-1}) are fixed. Using $\hat{y}^{(t)}$ to denote the predicted value at the t -th iteration of adding trees, xgboost minimizes the regularized loss $\mathcal{L}^{(t)}$ for the entire ensemble, as the scoring function in Equation (1).

$$\mathcal{L}^{(t)} = \sum_{i=1}^n l(y_i, \hat{y}^{(t)}) + \sum_{i=1}^t \Omega(f_i) \quad (3)$$

In the equation, l is an arbitrary loss function, e.g., cross entropy; and $\Omega(f_i)$ is the regularization term, which captures the complexity of the i -th tree, and encourages simpler trees to avoid overfitting.

Xgboost proposes the following regularization term, where T is the number of leaves in the t -th tree, w are the leaf weights used as the prediction, and γ and λ are hyperparameters.

$$\Omega(f_t) = \gamma T + \frac{1}{2} \lambda \|w\|^2 \quad (4)$$

The design of the regularization term by xgboost provides a closed form for the optimal leaf weights and minimal loss $\tilde{\mathcal{L}}_{struct}^{(t)}$ given the current tree structure, represented by T leaves where each leaf contains a set of training data points as I_j . In particular, $g_i = \partial_{\hat{y}^{(t-1)}}(l(y_i, \hat{y}^{(t-1)}))$, and $h_i = \partial_{\hat{y}^{(t-1)}}^2(l(y_i, \hat{y}^{(t-1)}))$ are the first order and second order gradients for the i -th data point.

$$\tilde{\mathcal{L}}_{struct}^{(t)} = -\frac{1}{2} \sum_{j=1}^T \left[\frac{(\sum_{i \in I_j} g_i)^2}{\sum_{i \in I_j} h_i + \lambda} \right] + \gamma T \quad (5)$$

Using the optimal solution (Equation (5)) as the scoring function for Equation (1), the gain can be computed as:

$$\begin{aligned} & \text{Gain}(I_L, I_R) \\ &= \frac{1}{2} \left[\frac{(\sum_{i \in I_L} g_i)^2}{\sum_{i \in I_L} h_i + \lambda} + \frac{(\sum_{i \in I_R} g_i)^2}{\sum_{i \in I_R} h_i + \lambda} - \frac{(\sum_{i \in I} g_i)^2}{\sum_{i \in I} h_i + \lambda} \right] - \gamma \end{aligned} \quad (6)$$

Boosting makes the newer tree dependent on previously grown trees. Previously, random forest was considered to

generalize better than gradient boosting, since boosting alone could overfit the training data without tree pruning, whereas bagging avoids that. The regularization term introduced by xgboost significantly improves the generalization of GBDT.

2.1.4 Feature Importance

Among non-linear classifiers with strong predictive power, tree ensembles offer unique model-level feature importance ranking. Once trained, random forest and gradient boosted decision tree models have the same model structure. Therefore, feature importance ranking can be computed in the same way.

There are mainly two ways to measure the feature importance in a tree ensemble, the mean increase gain (MIG) and mean decrease accuracy (MDA). Mean increase gain is commonly named as mean decrease impurity, originally proposed in [10] since the decrease in gini impurity has been used as the increase in gain. MIG adds up the weighted average gain for a feature in every tree, where the weight is the percentage of samples that are split by the feature. The mean decrease accuracy (MDA) [8, 9] measures the average decrease in accuracy of the ensemble, when the values of a feature are randomly permuted in out-of-bag samples (e.g., validation set). We use mean increase gain (MIG) as the feature importance measure in this paper, as evaluated by related work.

2.2 Evading Tree Ensembles

2.2.1 Threat Model

We evaluate the robustness of a tree ensemble by analyzing the potential evasion caused by the strongest whitebox adversary, the Mixed Integer Linear Program (MILP) attacker. The adversary has whitebox access to the model structure, model parameters and the prediction score.

2.2.2 MILP Attack

Strongest whitebox attack. Kantchelian et al. [27] have proposed to attack tree ensembles by constructing a mixed integer linear program, where the variables of the program are nodes of the trees, the objective is to minimize a distance (e.g., L_p norm distance) between the evasive example and the attacked data point, and the constraints of the program are based on the model structure. The constraints include model mislabel requirement, logical consistency among leaves and predicates. Using a solver, the MILP attack can find adversarial example with the *minimal evasion distance*. Otherwise, if the solver says the program is infeasible, there truly does not exist an adversarial example by perturbing the attacked data point. Since the attack is based on a linear program, we can use it to minimize any objective in the linear form.

Adversarial training limitation. The MILP attack cannot be efficiently used for adversarial training, e.g., it can take up to an hour to generate one adversarial example [12] depending on the model size. In addition, we want models to

learn knowledge about features. Therefore, we integrate the cost-driven constraint into the training process directly.

2.3 Related Work

Lowd and Meek [36] propose a linear attack cost function to model the feature importance. It is a weighted sum of absolute feature differences between the original data point and the evasive instance. Incer et al. [25] train monotonic classifiers with the assumption that the cost of decreasing some feature values is much higher compared to increasing them, such that attackers cannot evade by increasing feature values. In comparison, our cost-driven constraint is not restricted to the linear form, and we model difficulties in both increasing and decreasing feature values, since decreasing security features can incur costs of decreased utility [14, 28]. Zhang and Evans [51] are the first to train cost-sensitive robustness with regard to classification output error costs, since some errors have more catastrophic consequences than others [18]. Their work models the cost of classifier’s output, whereas we model the cost of perturbing the input features to the classifier.

There are several attacks against ensemble trees. The strongest whitebox attack is the Mixed Integer Linear Program (MILP) attack [27], which finds the exact minimal evasion distance to the model if an adversarial example exists. Another whitebox attack proposed by Papernot et al. [41] is based on heuristics. The attack searches for leaves with different classes within the neighborhood of the targeted leaf of the benign example, to find a small perturbation that results in a wrong prediction. Among the blackbox attacks, Cheng et al.’s attack [15] has been demonstrated to work on ensemble trees. The attack minimizes the distance between a benign example and the decision boundary, using a zeroth order optimization algorithm with the randomized gradient-free method.

3 Methodology

In this section, we present our methodology to train robust tree ensembles that utilize expert domain knowledge about features. We first describe how to specify the attack cost-driven constraint that capture the domain knowledge, then we describe our robust training algorithm utilizing the constraint, and lastly we propose a new objective for the adaptive attack to minimize the cost to evaluate the robust model.

3.1 Attack Cost-driven Constraint

3.1.1 Constraint Definition

We define the cost-driven constraint for each feature x^j to be $C(x^j)$. It is a mapping from the interval $[0, 1]$, containing normalized feature values, to a set in $[0, 1] \times [0, 1]$. For each concrete value of x^j , $C(x^j)$ gives the valid feature manipulation region according to the cost of changing the feature. For example, as indicated by the constraint in Figure 2, when $x^j = 0.7$ for one data point, the constraint says that the cost

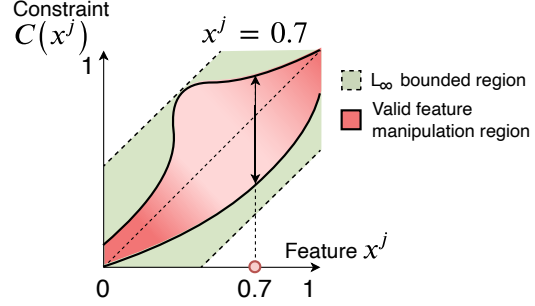


Figure 2: An example of cost-driven constraint for feature x^j . The red area valid the potential feature manipulation region under given cost-driven constraint $C(x^j)$ while the green area represents the common L_∞ -norm bounded region. Lighter red color means lower cost region, such that these feature values can be perturbed more by the attacker. The L_∞ region is imprecise to capture the cost.

is acceptable for the attacker to perturb x^j between 0.45 and 0.9. In general, the constraint can be anything specified by the domain expert. Next, we will describe factors that affect the cost, and give two example constraints.

3.1.2 Cost Factors

Economic: The economic return on the attacker’s investment is a major motivation to whether they are willing to change some features. For example, to evade blacklisting detection, the attackers constantly register new domains and rent new servers. Registering new domains is preferred since this costs less money than renting a new server.

Functionality: Some features are related to malicious functionalities of the attack. For example, the cryptojacking classifier [28] uses a feature that indicates whether the attack website calls the CryptoNight hashing function to mine Monero coins. It is a high cost to remove the hash function since the website can no longer mine Monero coins.

Suspiciousness: If the attacker needs to generate a lot more malicious activities to perturb features (e.g., sending more tweets than 99% of users), this makes the attack easier to be detected and has a cost.

Monotonicity: In security applications, the cost to increase a feature may be very different from decreasing it. For example, to evade malware detection that use “static import” features, it is easier to insert redundant libraries than to remove useful ones [25]. Therefore, we need to specify the cost for both directions of the change.

Attack seed: If the attack starts modifying features from a benign example (e.g., reverse mimicry attack), the cost of changing features may be different from modifying features

Cost	Value for l_j, h_j
Negligible	α
Low	β
Medium	γ
High	μ
Relationship	$\mu < \gamma < \beta < \alpha$

Table 1: Feature manipulation cost categories based on domain knowledge. For each feature j , we categorize the cost of increasing and decreasing its values and assign the bound for the box constraint using variables l_j and h_j .

from a malicious data point. Therefore, the classifier prediction of the seed can affect the cost.

3.1.3 Box Cost Constraint

We describe how to specify the box constraint to translate the security domain knowledge about features. For each feature, we categorize attacker’s cost of increasing and decreasing its value, into one of the four categories: negligible, low, medium, and high costs, based on relative cost differences, rather than absolute scale.

Negligible cost. There is negligible cost to perturb some features. For example, in the code transformation attack against authorship attribution classifier, the attacker can replace a for loop with a while loop without modifying any functionality of the code [44]. This changes the syntactic features of the classifier but incurs negligible costs.

Low and medium cost. Altering some features generates low or medium level of costs by comparison. For example, registering a new phishing domain name is generally considered to be lower cost for the attacker than renting and maintaining a new hosting server [34]. Therefore, increasing domain name count features can be categorized as low cost, whereas increasing IP address count features is medium cost.

High cost. If changing a feature significantly reduces the attack effectiveness, or compromises the attacker, then it is a high cost feature.

Box constraint. After assigning different categories to increasing/decreasing features, we can map the knowledge into a high dimensional box, to represent attacker’s preference of changing the features belonging to each category. Given m features, we have box constraint B formalized as $B = [-l_1, h_1] \times [-l_2, h_2] \times \dots \times [-l_d, h_d]$, where l_j, h_j denote the preferred lower and upper bound for the j -th feature value. Table 1 shows a mapping from the categories to four numerical values. All numerical values are between 0 and 1, representing the percentage of change with regard to the maximal value of the feature. A higher cost category should allow a smaller percentage of change than a lower cost category, to be consistent with the feature robustness knowledge. Specifically, $\mu < \gamma < \beta < \alpha$. The box constraint is a simple example of translating the domain knowledge about feature robustness into cost-driven constraint, that can be used in the training process.

Constraint. The box constraint corresponds to the following.

$$C(x^j) = [x^j - l_j, x^j + h_j], \quad j = 1, 2, 3, \dots, d \quad (7)$$

It means that for j -th feature, the constraint maps the feature to the interval $[x^j - l_j, x^j + h_j]$ that represents the amount of change as given the domain knowledge.

3.1.4 Conditioned Cost Constraint

We can use cost-driven constraint based on different conditions of the data point, e.g., the attack seed factor. In general, the constraint can vary for different feature values. For example, we can design the constraint in Equation (8) where x_i^j denotes the j -th feature value of data point x_i .

$$C(x_i^j) = \begin{cases} 0 & x_i \text{ is benign} \\ [x_i^j, 1] & x_i \text{ is mal, pred score} > 0.9 \\ [-0.1, 0.1] * x_i^j & x_i \text{ is mal, pred score} \leq 0.9 \end{cases} \quad (8)$$

In this example, we give different constraints for benign and malicious data points for the j -th feature. If a data point x_i is benign, we assign a value zero, meaning that it is extremely hard for the attacker to change the j -th feature value for a benign data point. If the data point is malicious, we separate to two cases. When the prediction score is higher than 0.9, we enforce that x_i^j can only be increased. On the other hand, when the prediction score is less than or equal to 0.9, we allow a relative 10% change for both increase and decrease directions, depending on the original value of x_i^j . Note that this is different from the box constraint proposed in Section 3.1.3. In the box constraint, we use the same percentage of change for a feature regardless of different feature values x_i^j . The cost-driven constraint allows us to capture and utilize all sorts of domain knowledge from security researchers, that is outside the training data.

3.2 Robust Training

Given attack cost-driven constraints specified by domain experts, we propose a new robust training algorithm that can integrate such information into the tree ensemble models.

3.2.1 Intuition

Using the box constraint as an example, we present the intuition of our robust training algorithm in Figure 3. The regular training algorithm of tree ensemble finds a non-robust split (top), whereas our robust training algorithm can find a robust split (bottom) given the attack cost-driven constraint. Specifically in the example, it is easier to decrease the feature x^j than to increase it. The cost constraint to increase (decrease) any x^j is defined by h_j (l_j). Here x_1, \dots, x_6 are six training points with two different labels. The top of Figure 3 shows

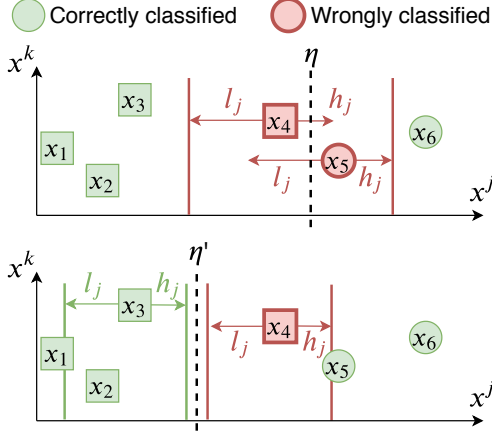


Figure 3: The intuition behind the attack cost-driven constraints for robust training, given six training points with two different classes (square and circle). It is easier to decrease x^j than to increase it for the attacker. In the top figure, the split is 100% accurate without attacks, but only 66.6% accurate under attacks. The split in the bottom figure is always robust, but has a 83.3% accuracy.

that, in regular training, the best split threshold η over feature x^j is between x_4 and x_5 , which perfectly separates the data points into left and right sets. However, given the attack cost to change feature x^j , x_4 and x_5 can both be easily perturbed by the adversary and cross the splitting threshold η . Therefore, the worst case accuracy under attacks is 66.6%, although the accuracy is 100% without attacks. By integrating the attack cost-driven constraints, we can choose a more robust split, as shown in the bottom of Figure 3. Even though the attacker can increase x_3^j by up to h_j , and decrease x_4^j by up to l_j , the data points cannot cross the robust split threshold η' . Therefore, the worst case accuracy under attacks is 83.3%, higher than that from the naive split. As a tradeoff, x_4 is wrongly separated without attacks, which makes the regular test accuracy 83.3% as well. As shown in the figure, using a robust split can increase the minimal evasion distance for the attacker to cross the split threshold.

3.2.2 Optimization Problem

In robust training, we want to maximize the gain computed from potential splits (feature j and threshold η), given the domain knowledge about how robust a feature x^j is. We use C to denote the attack cost-driven constraint. Following Equation (1), we have the following:

$$\begin{aligned}
 j^*, \eta^* &= \arg \max_{j, \eta} \text{Gain}(I_L, I_R, C) \\
 &= \arg \max_{j, \eta} (s(I, C) - s(I_L, I_R, C)) \\
 &= \arg \max_{j, \eta} (s(I) - s(I_L, I_R, C))
 \end{aligned} \tag{9}$$

Project constraint into set ΔI . Since the robustness of the feature does not change the score $s(I)$ before the split ($s(I, C)$

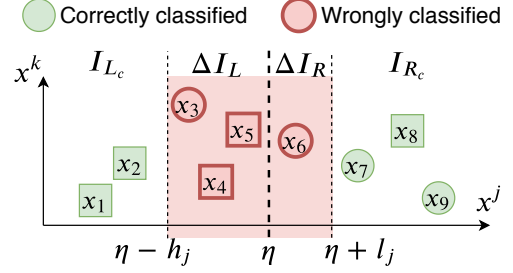


Figure 4: A simple example to illustrate the uncertain set $\Delta I = \Delta I_L \cup \Delta I_R = [x_3, x_4, x_5, x_6]$ within the robust region $[\eta - h_j, \eta + l_j]$ on feature x^j . Splitting threshold η splits the data points into high confidence left set $I_L = \Delta I_L \cup I_{Lc}$ and high confidence right set $I_R = \Delta I_R \cup I_{Rc}$. The data points within the uncertain set ΔI can be perturbed to cross the splitting threshold by attacks while the data points outside the uncertain set ($I_{Lc} \cup I_{Rc}$) are certain to be robust under any possible attacks.

is the same as $s(I)$), this only affects the score $s(I_L, I_R, C)$ after the split, which cannot be efficiently computed. Therefore, we project the second term as the worst case score conditioned on some training data points ΔI being perturbed given the constraint function. The perturbations degrade the quality of the split to two children sets I'_L and I'_R that are more impure or with higher loss values. To best utilize the feature robustness knowledge, we optimize for the maximal value of the score after the split, given different children sets I'_L and I'_R under the constraint:

$$\begin{aligned}
 s(I_L, I_R, C) &= \max_{I'_L, I'_R, C} s(I'_L, I'_R) \\
 &= \max_{\Delta I_L, \Delta I_R} s(I_{Lc} \cup \Delta I_L, I_{Rc} \cup \Delta I_R)
 \end{aligned} \tag{10}$$

Example. Different constraint functions result in different ΔI set. As an example, Figure 4 explains how we can map the box constraint for the j -th feature to an uncertain set ΔI containing variables to be optimized. We have nine data points numbered from 1 to 9, i.e. $I = \{x_1, x_2, \dots, x_9\}$, with two classes shaped in circles and squares. The training process tries to put the splitting threshold η between every two consecutive data points, in order to get the splitting point with maximum gain (Equation (1)). In Figure 4, the split value under consideration is between data points x_5 and x_6 . The regular training process then computes the gain of the split based on $I_L = \{x_1, x_2, x_3, x_4, x_5\}$ and $I_R = \{x_6, x_7, x_8, x_9\}$, using Equation 1. In the robust training process, we first project the box constraint for the feature $C(j) = [-l_j, h_j]$ into the set $\Delta I = \{x_3, x_4, x_5, x_6\}$. Since the points on the left side of threshold η can be increased up to h_j , and points on the right side of η can be decreased by up to l_j , we get the shaded region of $[\eta - h_j, \eta + l_j]$ containing four data points that can be perturbed to cross the splitting threshold η . Then, we need to maximize the score after split under the box constraint.

Combinatorial optimization. Given any constraint function and the split under consideration (j and η), we can calcu-

late the set of uncertain data points ΔI , the set of points that are certainly assigned to the left side I_{L_c} and the right side I_{R_c} , respectively. Each point in ΔI can be assigned to either the left side or the right side $\Delta I = \Delta I_L \cup \Delta I_R$, with $2^{|\Delta I|}$ possible assignments. Finding the minimal gain within all possible assignments is a combinatorial optimization problem. This becomes intractable as Equation (10) needs to be repeatedly solved during the training process. Therefore, to integrate feature robustness domain knowledge expressed in the constraint function, we need to efficiently solve Equation (10).

3.2.3 Robust Training Algorithm

We propose a new robust training algorithm to efficiently solve the optimization objective in Equation (10). Our algorithm works for different types of trees, including both classification and regression trees, different ensembles such as gradient boosted decision trees and random forest, and different splitting metrics used to compute the gain. Note that existing work can only support xgboost trees [11].

Algorithm 1 describes our robust training algorithm. The algorithm provides the optimal splitting features j^* and the splitting threshold η^* as output. The input includes the training dataset, the set of data points that reach the current node $I = \{(x_i, y_i)\}$, the attack cost-driven constraint function, and a score function s . Example score functions are the cross-entropy loss, Gini impurity, or Shannon entropy. From Line 10 to Line 28, the algorithm does robust training, and the loops outside that are the procedure used in regular training algorithm. The algorithm marches through every feature dimension (the for loop at Line 2), to compute the maximal score after the split given the feature robustness knowledge, for every possible split on that feature dimension. For each feature j , we first sort all the data points along that dimension (Line 3). Then, we go through all the sorted data points (x_{t_i}, y_{t_i}) to consider the gain of a potential split $x^j < \eta$ where η is calculated from Line 5 to Line 9. Given the constraint function C , we project that to the uncertain set ΔI and initialize two more sets: I_L contains the data points that stay on the left side of the split, and I_R contains the data points that stay on the right (Line 10 to 12). Next, from Line 13 to Line 22, we go through every uncertain data point, and greedily put it to either I_L or I_R , whichever gives a smaller gain for the current split. After that, we compute the gain at Line 24, and update the optimal split j^* , η^* for the current node if the current gain is the largest (Line 25 to 28). The algorithm eventually returns the optimal split (j^*, η^*) on Line 31.

3.3 Adaptive Attacker

To evaluate the robustness of a security classifier against adaptive attacker, we use the cost-driven constraint to improve the MILP attack objective. Specifically, we use the following optimization objective for the attacker under the box cost constraint to generate adversarial example \tilde{x} by perturbing x :

Algorithm 1 Robust Training Algorithm

Input: Training set $D = \{(x_i, y_i)\}, |D| = N (x_i \in \mathbb{R}^d, y \in \mathbb{R})$.

Input: data points of the current node $I = \{(x_i, y_i)\}, |I| = m$.

Input: attack cost-driven constraint C .

Input: the score function s .

Output: the best split at the current node j^*, η^* .

```

1: Initialize  $Gain^* = 0; j^* = 0; \eta^* = 0$ 
2: for  $j = 1$  to  $d$  do
3:   Sort  $I = \{(x_i, y_i)\}$  along the  $j$ -th feature as  $\{(x_{t_i}, y_{t_i})\}$ 
4:   for  $t_i = t_1$  to  $t_m$  do
5:     if  $t_i = t_1$  then
6:        $\eta \leftarrow x_{t_1}^j$ 
7:     else
8:        $\eta \leftarrow \frac{1}{2}(x_{t_i} + x_{t_{i-1}})$ 
9:     end if
10:    Project  $C$  to the uncertain set  $\Delta I$ .
11:     $I_L = \{(x_i, y_i) | x_i^j < \eta, x \notin \Delta I\}$ 
12:     $I_R = \{(x_i, y_i) | x_i^j > \eta, x \notin \Delta I\}$ 
13:    /* Greedily put  $(x_k, y_k)$  to whichever side that has a
14:       larger score. */
15:    for every  $(x_k, y_k)$  in  $\Delta I$  do
16:       $ls = s(I_L \cup \{(x_k, y_k)\}, I_R)$ 
17:       $rs = s(I_L, I_R \cup \{(x_k, y_k)\})$ 
18:      if  $ls < rs$  then
19:         $I_L = I_L \cup \{(x_k, y_k)\}$ 
20:      else
21:         $I_R = I_R \cup \{(x_k, y_k)\}$ 
22:      end if
23:    end for
24:    /* Find the maximal gain. */
25:     $Gain(j, \eta, I) = s(I) - s(I_L, I_R)$ 
26:    if  $Gain(j, \eta, I) > Gain^*$  then
27:       $j^* = j; \eta^* = \eta$ 
28:       $Gain^* = Gain(j, \eta, I)$ 
29:    end if
30:  end for
31: return  $j^*, \eta^*$ 

```

$$\text{minimize } \sum_j a_j u_j |\tilde{x}^j - x^j| + \sum_j (1 - a_j) v_j |\tilde{x}^j - x^j| \quad (11)$$

Where a_j is defined as the following:

$$a_j = \begin{cases} 0 & \tilde{x}^j \leq x^j \\ 1 & \tilde{x}^j > x^j \end{cases} \quad (12)$$

The cost objective is the weighted sum of absolute feature value differences, with different weights for the increase and decrease changes. Equation (11) uses weight u_j to scale the

change in the j -th feature if the feature is increased, and v_j to scale the decrease change, selected by the indicator variable a_j . We set weights u and v based on the inverse proportion of the box of each feature dimension, since a larger weight prefers a smaller feature change in the attack. This improves the strongest whitebox attack by including the knowledge of box constraint used in training. It minimizes the linear relation of attack costs using the domain knowledge.

4 Evaluation

In this section, we first evaluate the effectiveness of our core training technique (Section 4.2), and then we evaluate the end-to-end robust training method on a security task, twitter spam detection (Section 4.3).

4.1 Implementation

We implement our robust training algorithm in xgboost [13] and scikit-learn [4]. The implementation in xgboost works with all their supported differentiable loss functions for gradient boosted decision trees. For scikit-learn, we implement the robust training algorithm in random forest using the gini impurity score.

4.2 Training Algorithm Evaluation

Since the state-of-the-art training method [11] does not support cost model other than L_∞ -norm, we compare our core training algorithm (Algorithm 1) against existing work without any domain knowledge related cost modeling in this section. Even though it is unfair to our technique, the experiments in this section act as an ablation study to show the improvements our Algorithm 1 makes to solve Equation (10). Same as [11], we run our Algorithm 1 to train L_∞ -norm bounded robustness as proposed in related work for each dataset.

4.2.1 Benchmark Datasets

We evaluate the robustness improvements in 4 benchmark datasets: breast cancer, cod-rna, ijcn1, and binary MNIST (2 vs. 6). The size of the training/testing sets and the number of features for these datasets are shown in Table 4. For consistency, we follow the same experiment settings used in [11], including number of trees, maximum depth, and trained ϵ for L_∞ -norm bound. Same as [11], we randomly shuffle the test set, and generate adversarial examples for 100 test data points for breast cancer, ijcn1, and binary MNIST, and 5000 test points for cod-rna. We describe the details of each benchmark dataset below.

breast cancer. The breast cancer dataset [1] contains 2 classes of samples, each representing benign and malignant cells. The attributes represent different measurements of the cell’s physical properties (e.g., the uniformity of cell size/shape).

cod-rna. The cod-rna dataset [2] contains 2 classes of samples representing sequenced genomes, categorized by the existence

of non-coding RNAs. The attributes contain information on the genomes, including total free-energy change, sequence length, and nucleotide frequencies.

ijcn1. The ijcn1 dataset [3] is from the IJCNN 2001 Neural Network Competition. Each sample represents the state of a physical system at a specific point in a time series, and has a label indicating “normal firing” or “misfiring”. The original 5 attributes in each sample are measurements of different properties of the physical system. Here, we use the 22-attribute version of ijcn1, a transformation of original data, since it turned out to achieve the best performance and won the competition.

MNIST 2 vs. 6. The binary mnist dataset [5] contains handwritten digits of “2” and “6”. The attributes represent the gray levels on each pixel location.

L_∞ robustness definition. When the objective of the MILP attack (Section 2.2.2) is to minimize the L_∞ distance, the attack provides the *minimal L_∞ -norm distance* that the attacker needs to perturb in the features in order to evade the model. In non-security related applications, a larger L_p robustness distance means that a model is more robust. For example, if the MNIST classifier requires an average of 0.3 L_∞ norm distance changes in adversarial examples, the adversarial examples look more differently from the original image, compared to evading the baseline model with 0.06 L_∞ norm robustness distance. Therefore, the former model is more robust.

4.2.2 GBDT Results

We first evaluate the robustness of our training algorithm on the gradient boosted decision trees (GBDT) models with the four aforementioned benchmark datasets. We measure the model robustness with the average L_∞ distance of the adversarial examples found by Kantchelian et al.’s MILP attack [27]. Note that Kantchelian’s MILP attack is the strongest whitebox attack under L_p -norm robustness distance for tree ensemble models. We compare the robustness of the model trained with our robust algorithm against those trained from the regular training algorithm, as well as the state-of-the-art robust training algorithm proposed by Chen et al. [11].

As shown in Table 2, the GBDT models trained with our robust algorithms are more robust than the ones trained with regular training method and state-of-the-art robust training method. Specifically, it costs the Kantchelian et al.’s MILP attack $2.94\times$ more L_∞ perturbation distance to evade our GBDT models than regularly trained ones. Compared to the state-of-the-art Chen and Zhang et al.’s robust training method [11], our models require on average $1.26\times$ larger L_∞ perturbation distances while our models still maintain relatively high accuracy and low false positive rate. Note that the robustness improvement of our trained models are limited on binary MNIST dataset. This is because the trained and tested robustness ranges $L_\infty \leq 0.3$ are fairly large for MNIST dataset. The adversarial examples beyond that range are not imperceptible

Dataset	# of trees	Trained ϵ		Tree Depth			Test ACC (%)			Test FPR (%)			Avg. l_∞			Improv.	
		Chen's	ours	natural	Chen's	ours	natural	Chen's	ours	natural	Chen's	ours	natural	Chen's	ours	natural	Chen's
breast-cancer	4	0.30	0.30	6	8	8	98.54	97.81	96.35	0.98	0.98	0.98	.2096	.3938	.5146	2.58x	1.31x
cod-rna	20	0.20	0.03	4	5	5	96.48	88.09	88.03	2.57	4.44	7.59	.0343	.0560	.0692	2.02x	1.24x
ijcnn1	60	0.20	0.02	8	8	8	97.91	96.03	93.65	1.64	2.15	1.62	.0268	.0326	.0463	1.73x	1.42x
MNIST 2 vs. 6	1,000	0.30	0.30	4	6	6	99.75	99.54	99.54	0.39	3.88	3.88	.0609	.3132	.3308	5.43x	1.06x

Table 2: Test accuracy and robustness of GBDT models trained by our algorithm (ours), compared to regularly trained models (natural) and the models trained by Chen and Zhang et al.’s method [11] (Chen’s), in xgboost. We evaluate the model robustness with the average l_∞ distance of the adversarial examples found by Kantchelian’s MILP attack [27], the strongest whitebox attack. The improvement (Improv.) here denotes the average l_∞ robustness distance on our models over regularly trained ones and Chen and Zhang’s.

Dataset	# of trees	Trained ϵ		Tree Depth		Test ACC (%)		Test FPR (%)		Avg. l_∞		Improv. natural
		ours	natural	ours	natural	ours	natural	ours	natural	ours		
breast-cancer	20	0.30	6	6	99.27	99.27	0.98	0.98	.2091	.3783	1.81x	
cod-rna	60	0.20	14	14	96.55	89.11	2.97	5.28	.0437	.0686	1.57x	
ijcnn1	80	0.10	14	14	97.90	92.24	1.54	0.06	.0278	.1151	4.14x	
MNIST 2 vs. 6	60	0.30	14	14	99.55	99.30	0.38	0.48	.0484	.2558	5.29x	

Table 3: Test accuracy and robustness of random forest models trained by our algorithm (ours) compared to regularly trained models (natural), in scikit-learn. The improvement (Improv.) here denotes the average l_∞ robustness distance on our models over regularly trained ones.

Dataset	Train set size	Test set size	# of features
breast-cancer	546	137	10
cod-rna	59,535	271,617	8
ijcnn1	49,990	91,701	22
MNIST 2 vs. 6	11,876	1,990	784

Table 4: Training and testing set sizes, and number of features for the four benchmark datasets.

any more and thus the robustness becomes extremely hard to achieve without heavily sacrificing regular accuracy.

4.2.3 Random Forest Results

In this subsection, we evaluate the robustness of random forest models trained with our robust algorithms on the four benchmark datasets. We implement our algorithm in a commonly used library scikit-learn [4]. to the best of our knowledge, no robust training methods are available under that setting using traditional gain metrics such as gini impurity and shannon entropy. Thus, we only compare against regular training algorithm for random forest models. We also measure the robustness of random forest models with the average L_∞ distance of adversarial examples found by Kantchelian et al.’s MILP attack [27].

As shown in Table 3, the robustness of our random forest models significantly outperforms the regularly trained ones. Specifically, the average l_∞ distance of adversarial examples found by Kantchelian et al.’s MILP attack [27] is on average $3.2\times$ larger than regular ones. On the other hand, there is only a 3.3% drop of test accuracy and a 0.2% increase of false positive rate on average for the robust models, although the underlying optimization is much harder for robust training than regular training.

4.2.4 Benefits of our robust algorithms over existing heuristics

Here, we move one step further to provide insights on why our robust training algorithm outperforms the state-of-the-art Chen and Zhang et al.’s [11] and baseline training methods as shown in Section 4.2.2 and 4.2.3. Essentially, the robustness improvement mainly benefits from our proposed robust algorithm in solving the maximization problem of Equation (10).

According to Equation (10), our robust algorithm is designed to maximize some impurity measure for each potential feature split during the training process. The higher the score is obtained by the algorithm, the stronger capability of the attacker is used for training, which guides the model to learn stronger robustness. Therefore, how well the algorithm can solve the maximization problem directly determines the eventual robustness the models can learn. To that end, we measure how our robust algorithm performs in solving the maximization problem compared to the heuristics used in state-of-the-art Chen and Zhang’s training algorithms [11] to illustrate its effectiveness.

Dataset	Better (%)	Equal (%)	Worse (%)	Total
breast-cancer	99.74	0.26	0	3,047
cod-rna	94.13	4.66	1.21	35,597
ijcnn	90.31	1.11	8.58	424,825
MNIST 2 vs. 6	87.98	6.33	5.69	796,264

Table 5: The percentage of the cases where our robust algorithm performs better, equally well, or worse than the heuristics used in the state-of-the-art Chen and Zhang et al.’s robust training algorithms [11] in solving the maximization problem (Equation 10). The total number of cases represent the total number of splits evaluated during robust optimization.

On the four benchmark datasets, we measure the percentage of the cases where our robust algorithms can better solve the maximization problem than the heuristics used in [11] and summarize the results in Table 5. The results show that our robust algorithm can provide a better solution than heuristics used in Chen and Zhang et al.’s method [11] for at least 87.98% cases during the whole training process. On small datasets like breast-cancer and cod-rna, our algorithm performs equally or better for 100% and 98.79% cases respectively. Such significant improvements in solving the maximization problem greatly benefit the robustness of our trained models. The results provide insights on why our robust training algorithm can obtain more robust tree ensembles than existing training methods.

4.3 Twitter Spam Detection Application

In this section, we apply our robust tree ensemble training method to a classic security application, spam URL detection on Twitter [32]. As a case study for security classifiers, we want to answer the following questions in the evaluation:

- **Cost-driven constraint:** How to specify the cost-driven constraint based on security domain knowledge?
- **Model explainability:** Does the robust model prefer more robust features compared to the baseline model?
- **Economic cost:** Against the strongest whitebox attack [27], does the robust model increase the economic cost for the adaptive attacker to evade it?

4.3.1 Dataset

We obtain the public dataset used in Kwon et al.’s work [32] to detect spam URLs posted on Twitter. Spammers spread harmful URLs on social networks such as Twitter to distribute malware, scam, or phishing content. These URLs go through a series of redirections, and eventually reach a landing page containing harmful content. The existing detectors proposed in prior works often make decisions based on content-based features that are strong in predictive power but easy to be changed, e.g., different words used in the spam tweet. Kwon et al. propose to use more robust features that incur monetary or management cost to be changed under adversarial settings. They extract these robust features from the URL redirection chains (RC) and the corresponding connected components (CC) formed by the chains.

Dataset	Training	Testing
Malicious	130,794	55,732
Benign	165,076	71,070
Total	295,870	126,802

Table 6: The size of Twitter spam dataset [32].

Feature extraction. We reimplemented and extracted 25 features from the dataset in the original paper, as shown in

Table 7. There are four families of features: shared resources-driven, heterogeneity-driven, flexibility-driven, and user account and post level features. The key intuitions behind the features are as follows. 1) Attackers reuse underlying hosting infrastructure to reduce the economic cost of renting and maintaining servers. 2) Attackers use machines hosted on bulletproof hosting services or compromised machines to operate the spam campaigns. These machines are located around the world, which tend to spread over larger geographical distances than benign hosting infrastructure, and it is hard for attackers to control the geographic location distribution of their infrastructure. 3) Attackers want to maximize the flexibility of the spam campaign, so they use many different initial URLs to make the posts look distinct, and different domains in the long redirection chains to be agile against takedowns. 4) Twitter spammers utilize specific characters to spread harmful content, such as hashtags and ‘@’ mentions. We removed some highly correlated features from the original paper. For example, for a feature where the authors use both maximum and average numbers, we use the average number only.

Kwon et al. labeled the dataset by crawling suspended users, identifying benign users, and manually annotating tweets and URLs. In total, there are 186,526 distinct malicious tweets with spam URLs, and 236,146 benign ones. We randomly split the labeled dataset into 70% training set and 30% testing set as shown in Table 6. We extract the aforementioned 25 features from each data point and normalize the values to be between 0 and 1 for training and testing.

4.3.2 Cost-driven Constraint

In order to obtain the cost-driven constraint for robust training, we first analyze the cost of changing the features and the direction of the changes, then we specify a box constraint for the cost accordingly.

Feature Analysis We categorize the features into low, medium, and high cost to change, as shown in Table 7. We analyze the cost based on feature families as follows.

- **Shared resources:** All features cost more to be decreased than to be increased. If the attacker does not reuse the redirector in the chain as much as before, the attacker needs to set up additional redirector servers to maintain the same level of spam activities (EntryURLid and AvgURLid features). It costs even more to set up more servers for the landing pages, since the landing URLs contain actual malicious content, which are usually hosted on bulletproof hosting (BPH) services. Feature AvgLdURLDom captures how the attacker is reusing the malicious content hosting infrastructure. If the value is decreased, the attacker will need to set up more BPH servers, which has the highest cost in the category.
- **Heterogeneity:** The total geographical distance traversed by the URL nodes in the redirection chain has the highest

Feature Name	Description	Cost		Constraint	Cost Weight	
		Decrease	Increase	Variables (l_i, h_i)	u_i	v_i
Shared Resources-driven Features						
EntryURLid	In degree of the largest redirector	Medium	Negligible	(-0.05, 0.2)	4	1
AvgURLid	Average in degree of URL nodes in the RC	Medium	Negligible	(-0.05, 0.2)	4	1
ChainWeight	Total frequency of edges in the RC	Low	Negligible	(-0.1, 0.2)	2	1
CCsize	# of nodes in the CC	Low	Negligible	(-0.1, 0.2)	2	1
CCdensity	Edge density of the CC	Low	Negligible	(-0.1, 0.2)	2	1
MinRCLen	Min length of the RCs in the CC	Low	Negligible	(-0.1, 0.2)	2	1
AvgLdURLDom	Average domain # of landing URL IPs in the CC	High	Negligible	(0, 0.2)	∞	1
AvgURLDom	Average domain # for the IPs in the RC	Medium	Negligible	(-0.05, 0.2)	4	1
Heterogeneity-driven Features						
GeoDist	Total geo distance (km) traversed by the RC	High	Negligible	(0, 0.2)	∞	1
CntContinent	# of unique continents in the RC	Medium	Negligible	(-0.05, 0.2)	4	1
CntCountry	# of unique countries in the RC	Medium	Negligible	(-0.05, 0.2)	4	1
CntIP	# of unique IPs in the RC	Low	Negligible	(-0.1, 0.2)	2	1
CntDomain	# of unique domains in the RC	Low	Negligible	(-0.1, 0.2)	2	1
CntTLD	# of unique TLDs in the RC	Low	Negligible	(-0.1, 0.2)	2	1
Flexibility Features						
ChainLen	Length of the RC	Low	Negligible	(-0.1, 0.2)	2	1
EntryURLDist	Distance from initial URL to the largest redirector	Low	Negligible	(-0.1, 0.2)	2	1
CntInitURL	# of initial URLs in the CC	Low	Negligible	(-0.1, 0.2)	2	1
CntInitURLDom	Total domain name # in the initial URLs	Low	Negligible	(-0.1, 0.2)	2	1
CntLdURL	# of final landing URLs in the RC	Low	Negligible	(-0.1, 0.2)	2	1
AvgIPperURL	Average IP # per URL in the RC	Low	Negligible	(-0.1, 0.2)	2	1
AvgIPperLdURL	Average IP # per landing URL in the CC	Low	High	(-0.1, 0)	2	∞
User Account Features						
Mention Count	# of '@' count to mention other users	Negligible	Low	(-0.2, 0.1)	1	2
Hashtag Count	# of hashtags	Negligible	Low	(-0.2, 0.1)	1	2
Tweet Count	# of tweets made by the user account	Negligible	Medium	(-0.2, 0.05)	1	4
URL Percent	Percentage of user posts that contain a URL	Negligible	Low	(-0.2, 0.1)	1	2

*CC: connected component. RC: redirection chain. BPH: bulletproof hosting.

Table 7: We reimplement 25 features used in [32] to detect twitter spam, among which three features have high cost to decrease or increase. To maintain the same level of spam activities, the attacker needs to purchase more bulletproof hosting servers to host the different landing pages if AvgLdURLDom feature is decreased or AvgIPperLdURL feature is increased. In addition, it is very hard for the attacker to decrease the GeoDist feature. The last two columns assign the weights in Equation (11) used to minimize attack cost for the adaptive attacker.

cost to change in general (GeoDist). If the attacker uses all the available machines as resources for malicious activities, it is hard to control the location of the machines and the distance between them. Overall, it is harder to decrease GeoDist to what looks more like benign value than to increase it. Since GeoDist values for benign URL redirection chains are very concentrated in one or two countries, the attacker would need to purchase more expensive resources located close by to mimic benign URL. The other four features that count number of continents, countries, IPs, domains, and top-level domains incur cost for decreased flexibility and increased maintainence cost if the features are decreased.

- **Flexibility:** All features in this family except the last one have relatively low cost to decrease, because that decreases the flexibility of the attack. The high cost feature AvgIPperLdURL counts the number of IP addresses that host the malicious landing page URL. If the attacker wants more flexibility of hosting the landing page on more BPH servers, the cost will be increased significantly.
- **User account:** Increasing features in this family generally

increases suspiciousness of the user account. Among them, increasing the tweet count is the most suspicious of all, since a tweet is capped by 140 characters which limits the number of mentions and hashtags, and percentage of posts containing URLs is also capped. If a user account sends too many tweets that puts the account to the top suspicious percentile, it can be easily detected by simple filtering mechanism and compromise the account.

Overall, three features have the highest cost to be perturbed: AvgLdURLDom, GeoDist², and AvgIPperLdURL. Decreasing AvgLdURLDom and increasing AvgIPperLdURL incurs cost to obtain more bulletproof hosting servers for the landing page URL, and manipulating GeoDist is generally outside the control of the attacker. Other types of actions can also achieve the changes in AvgLdURLDom and AvgIPperLdURL, but it will generally decrease the profit of the malicious operation. To decrease AvgLdURLDom, if the attacker does not rent more BPH servers but only reduces the number of malicious landing pages, that reduces the profit. If the attacker increases

²GeoDist, CntContinent and CntCountry have similar intuition, but we choose GeoDist since it has finer granularity in feature values.

Model	Cost Aware	Cost Model	# of trees	Tree Depth	ACC (%)	FPR (%)	Avg. Evasion Cost	Improv.
Regular Training	No	N/A	30	8	99.38	0.89	0.010	N/A
Our Robust Model	Yes	Cost-driven constraint	150	24	96.96	4.1	0.064	6.4x

Table 8: Robustness improvement of twitter spam classification models. We use our new training algorithm to train a robust gradient boosted decision trees model, and compare it against the baseline model. Results show that we achieve 6.4 \times evasion cost increase against the adaptive whitebox attacker [27] who minimizes the attack cost (Equation (11)).

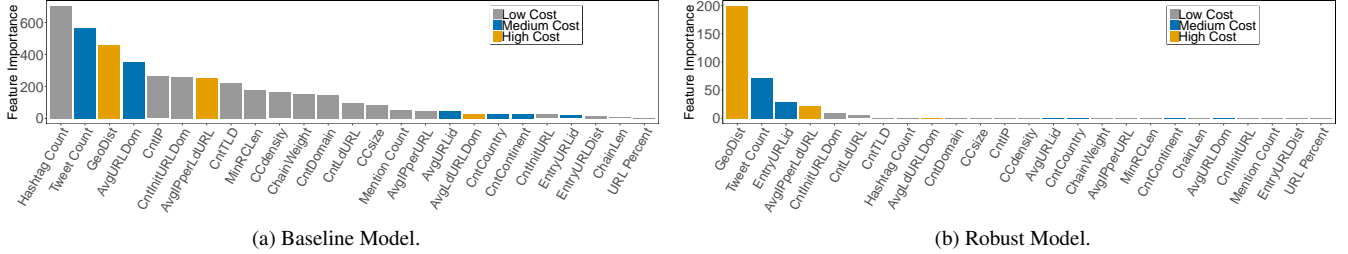


Figure 5: The robust model ranks medium cost and high cost features higher than the baseline model. All three high cost features are ranked within top ten most important features for the robust model.

the AvgIPperLdURL by using cheap servers, their malicious content could be taken down more often that interrupts the malicious operation.

Box Constraint Specification. We want to allow more perturbations for low cost features than high cost ones, and more perturbations on the low cost side (increase or decrease) than the more costly side. So we give larger ranges for low cost features, with direction of the ranges. We specify box constraint according to Section 3.1.3 using the following values: $\alpha = 0.2, \beta = 0.1, \gamma = 0.05, \mu = 0$. The corresponding perturbation ranges for each feature is shown in the Constraint Variables column in Table 7.

4.3.3 Robust Model

Using the cost-driven constraint, we trained a robust gradient boosted decision trees using our implementation in xgboost. We compare against the baseline model trained by the regular GBDT training method as shown in Table 8.

Model performance: our robust model has reasonable performance while it can learn robustness under cost-driven constraint. We achieve 96.96% accuracy and 4.1% false positive rate by increasing the number of trees and maximum tree depth used in the robust training process (Table 8). It is a known tradeoff that increasing the robustness of a classifier may decrease its regular test accuracy and increase the false positive rate. In security applications, it is especially important to maintain low false positive rate to reduce the number of false alarms. Under some cost constraint settings, e.g., using (0, 0) as variables for the high cost features AvgLdURL-Dom, GeoDist, and AvgIPperLdURL, we can train a model with 2.9% FPR. Improving the false positive rate of the robust model will be a direction for future work.

Feature importance ranking: our robust model ranks high cost features as most importance ones, compared to the baseline models. Figure 5 shows that the model trained using our robust training algorithm ranks high cost features

as more important ones, compared to the baseline model. The feature importance score is computed by the mean increase gain (MIG, described in Section 2.1.4), that averages the contribution of the loss reduction for splitting on the specific features across the ensemble. Figure 5a shows that the baseline model heavily relies on the Hashtag Count feature, such that it has a very high feature importance score. Within top ten most important features for the baseline model, six of them are low cost features, and only one is high cost feature. On the other hand, Figure 5b shows that all three high cost features are within the top ten, and they rank much higher in the robust model than the baseline model.

Robustness increase against adaptive attacker: our robust model can cause the attacker 6.4 \times times cost increase for evasion compared to the baseline model. To evaluate the robustness, we run the strongest whitebox MILP attack [27] that minimizes the cost objective of feature changes (Equation (11)). We run the attack from 100 randomly selected malicious test data points. By perturbing the malicious points, the attack finds the exact minimal cost to generate adversarial examples for these data. On average, our robust model obtains 6.4 \times increase in the minimal cost compared to the baseline.

Other attacks. MILP attack is the strongest whitebox attack against tree ensembles. We minimize the attack cost of evasion, by setting the feature weights in the cost function according to the same proportion used in the training (Equation (11) and Table 7). Therefore, this adaptive attack directly targets the training technique. Stronger attacks require a more complicated modeling of the evasion cost, which needs to consider indirect cost not captured by the features, e.g., profit of different malicious activity levels, change of suspiciousness and chances of being detected, etc. We plan to explore these as future work.

5 Conclusion

In this paper, we have designed, implemented, and evaluated a cost-aware robust training method to train tree ensembles for security. We have proposed a cost modeling method to capture the domain knowledge about features, and a robust training algorithm to integrate such knowledge. Using our method, we have trained a robust twitter spam detection model that prefers high cost features than low cost ones, while maintaining reasonable performance. Moreover, our robust model can increase the attack evasion cost by $6.4\times$ against the adaptive attacker.

References

- [1] Breast Cancer Wisconsin (Original) Data Set. [https://archive.ics.uci.edu/ml/datasets/breast+cancer+wisconsin+\(original\)](https://archive.ics.uci.edu/ml/datasets/breast+cancer+wisconsin+(original)).
- [2] Cod-RNA Data Set. <https://www.csie.ntu.edu.tw/~cjlin/libsvmtools/datasets/binary.html#cod-rna>.
- [3] Ijcnn1 Data Set. <https://www.csie.ntu.edu.tw/~cjlin/libsvmtools/datasets/binary.html#ijcnn1>.
- [4] scikit-learn: Machine Learning in Python. <https://scikit-learn.org/>.
- [5] The MNIST Database of Handwritten Digits. <http://yann.lecun.com/exdb/mnist/>.
- [6] M. Andriushchenko and M. Hein. Provably robust boosted decision stumps and trees against adversarial attacks. In *Advances in Neural Information Processing Systems*, pages 12997–13008, 2019.
- [7] L. Breiman. Bagging predictors. *Machine learning*, 24(2):123–140, 1996.
- [8] L. Breiman. Random forests. *Machine learning*, 45(1):5–32, 2001.
- [9] L. Breiman. Manual on setting up, using, and understanding random forests v3. 1. *Statistics Department University of California Berkeley, CA, USA*, 1:58, 2002.
- [10] L. Breiman, J. Friedman, R. Olshen, and C. Stone. Classification and regression trees. *Wadsworth Int Group*, 37(15):237–251, 1984.
- [11] H. Chen, H. Zhang, D. Boning, and C.-J. Hsieh. Robust decision trees against adversarial examples. In *International Conference on Machine Learning (ICML)*, 2019.
- [12] H. Chen, H. Zhang, S. Si, Y. Li, D. Boing, and C.-J. Hsieh. Robustness verification of tree-based models. In *Advances in Neural Information Processing Systems*, 2019.
- [13] T. Chen and C. Guestrin. Xgboost: A scalable tree boosting system. In *Proceedings of the 22nd acm sigkdd international conference on knowledge discovery and data mining*, pages 785–794. ACM, 2016.
- [14] Y. Chen, Y. Nadji, A. Kountouras, F. Monrose, R. Perdisci, M. Antonakakis, and N. Vasiloglou. Practical attacks against graph-based clustering. In *Proceedings of the 2017 ACM SIGSAC Conference on Computer and Communications Security*, pages 1125–1142. ACM, 2017.
- [15] M. Cheng, T. Le, P.-Y. Chen, J. Yi, H. Zhang, and C.-J. Hsieh. Query-efficient hard-label black-box attack: An optimization-based approach. In *International Conference on Learning Representations (ICLR)*, 2019.
- [16] A. Cidon, L. Gavish, I. Bleier, N. Korshun, M. Schweighauser, and A. Tsitkin. High precision detection of business email compromise. In *28th {USENIX} Security Symposium ({USENIX} Security 19)*, pages 1291–1307, 2019.
- [17] J. M. Cohen, E. Rosenfeld, and J. Z. Kolter. Certified adversarial robustness via randomized smoothing. *arXiv preprint arXiv:1902.02918*, 2019.
- [18] T. Dreossi, S. Jha, and S. A. Seshia. Semantic adversarial deep learning. *arXiv preprint arXiv:1804.07045*, 2018.
- [19] K. Dvijotham, S. Gowal, R. Stanforth, R. Arandjelovic, B. O’Donoghue, J. Uesato, and P. Kohli. Training verified learners with learned verifiers. *arXiv preprint arXiv:1805.10265*, 2018.
- [20] I. Fette, N. Sadeh, and A. Tomasic. Learning to detect phishing emails. In *Proceedings of the 16th international conference on World Wide Web*, pages 649–656. ACM, 2007.
- [21] Y. Freund. Boosting a weak learning algorithm by majority. *Information and computation*, 121(2):256–285, 1995.
- [22] Y. Freund and R. E. Schapire. A decision-theoretic generalization of on-line learning and an application to boosting. *Journal of computer and system sciences*, 55(1):119–139, 1997.
- [23] S. Gowal, K. Dvijotham, R. Stanforth, R. Bunel, C. Qin, J. Uesato, T. Mann, and P. Kohli. On the effectiveness of interval bound propagation for training verifiably robust models. *arXiv preprint arXiv:1810.12715*, 2018.

- [24] G. Ho, A. Cidon, L. Gavish, M. Schweighauser, V. Paxson, S. Savage, G. M. Voelker, and D. Wagner. Detecting and characterizing lateral phishing at scale. In *28th {USENIX} Security Symposium ({USENIX} Security 19)*, pages 1273–1290, 2019.
- [25] I. Incer, M. Theodorides, S. Afroz, and D. Wagner. Adversarially robust malware detection using monotonic classification. In *Proceedings of the Fourth ACM International Workshop on Security and Privacy Analytics*, pages 54–63. ACM, 2018.
- [26] U. Iqbal, P. Snyder, S. Zhu, B. Livshits, Z. Qian, and Z. Shafiq. Adgraph: A graph-based approach to ad and tracker blocking. In *Proc. of IEEE Symposium on Security and Privacy*, 2020.
- [27] A. Kantchelian, J. Tygar, and A. Joseph. Evasion and hardening of tree ensemble classifiers. In *International Conference on Machine Learning*, pages 2387–2396, 2016.
- [28] A. Kharraz, Z. Ma, P. Murley, C. Lever, J. Mason, A. Miller, N. Borisov, M. Antonakakis, and M. Bailey. Outguard: Detecting in-browser covert cryptocurrency mining in the wild. In *The World Wide Web Conference*, pages 840–852, 2019.
- [29] A. Kharraz, W. Robertson, and E. Kirda. Surveylance: automatically detecting online survey scams. In *2018 IEEE Symposium on Security and Privacy (SP)*, pages 70–86. IEEE, 2018.
- [30] M. Konte, R. Perdisci, and N. Feamster. Aswatch: An as reputation system to expose bulletproof hosting ases. *ACM SIGCOMM Computer Communication Review*, 45(4):625–638, 2015.
- [31] B. J. Kwon, J. Mondal, J. Jang, L. Bilge, and T. Dumitraş. The dropper effect: Insights into malware distribution with downloader graph analytics. In *Proceedings of the 22nd ACM SIGSAC Conference on Computer and Communications Security*, pages 1118–1129. ACM, 2015.
- [32] H. Kwon, M. B. Baig, and L. Akoglu. A domain-agnostic approach to spam-url detection via redirects. In *Pacific-Asia Conference on Knowledge Discovery and Data Mining*, pages 220–232. Springer, 2017.
- [33] M. Lecuyer, V. Atlidakis, R. Geambasu, D. Hsu, and S. Jana. Certified robustness to adversarial examples with differential privacy. In *2019 IEEE Symposium on Security and Privacy (SP)*, pages 656–672. IEEE, 2019.
- [34] K. Levchenko, A. Pitsillidis, N. Chachra, B. Enright, M. Félegyházi, C. Grier, T. Halvorson, C. Kanich, C. Kreibich, H. Liu, et al. Click trajectories: End-to-end analysis of the spam value chain. In *2011 IEEE Symposium on Security and Privacy*, pages 431–446. IEEE, 2011.
- [35] B. Li, C. Chen, W. Wang, and L. Carin. Second-order adversarial attack and certifiable robustness. 2018.
- [36] D. Lowd and C. Meek. Adversarial Learning. In *Proceedings of the eleventh ACM SIGKDD international conference on Knowledge discovery in data mining*, pages 641–647. ACM, 2005.
- [37] A. Madry, A. Makelov, L. Schmidt, D. Tsipras, and A. Vladu. Towards deep learning models resistant to adversarial attacks. *International Conference on Learning Representations (ICLR)*, 2018.
- [38] M. Mirman, T. Gehr, and M. Vechev. Differentiable abstract interpretation for provably robust neural networks. In *International Conference on Machine Learning (ICML)*, pages 3575–3583, 2018.
- [39] T. Nelms, R. Perdisci, M. Antonakakis, and M. Ahamad. Towards measuring and mitigating social engineering software download attacks. In *25th {USENIX} Security Symposium ({USENIX} Security 16)*, pages 773–789, 2016.
- [40] M. Norouzi, M. Collins, M. A. Johnson, D. J. Fleet, and P. Kohli. Efficient non-greedy optimization of decision trees. In *Advances in neural information processing systems*, pages 1729–1737, 2015.
- [41] N. Papernot, P. McDaniel, and I. Goodfellow. Transferability in machine learning: from phenomena to black-box attacks using adversarial samples. *arXiv preprint arXiv:1605.07277*, 2016.
- [42] J. R. Quinlan. Induction of decision trees. *Machine learning*, 1(1):81–106, 1986.
- [43] J. R. Quinlan. C 4.5: Programs for machine learning. *The Morgan Kaufmann Series in Machine Learning*, 1993.
- [44] E. Quiring, A. Maier, and K. Rieck. Misleading authorship attribution of source code using adversarial learning. In *28th {USENIX} Security Symposium ({USENIX} Security 19)*, pages 479–496, 2019.
- [45] M. Z. Rafique, T. Van Goethem, W. Joosen, C. Huygens, and N. Nikiforakis. It’s free for a reason: Exploring the ecosystem of free live streaming services. In *Proceedings of the 23rd Network and Distributed System Security Symposium (NDSS 2016)*, pages 1–15. Internet Society, 2016.
- [46] R. E. Schapire. The strength of weak learnability. *Machine learning*, 5(2):197–227, 1990.

- [47] A. Sinha, H. Namkoong, and J. Duchi. Certifying some distributional robustness with principled adversarial training. *International Conference on Learning Representations (ICLR)*, 2018.
- [48] S. Wang, Y. Chen, A. Abdou, and S. Jana. Mixtrain: Scalable training of formally robust neural networks. *arXiv preprint arXiv:1811.02625*, 2018.
- [49] E. Wong and Z. Kolter. Provable defenses against adversarial examples via the convex outer adversarial polytope. In *International Conference on Machine Learning*, pages 5283–5292, 2018.
- [50] E. Wong, F. Schmidt, J. H. Metzen, and J. Z. Kolter. Scaling provable adversarial defenses. *Advances in Neural Information Processing Systems (NIPS)*, 2018.
- [51] X. Zhang and D. Evans. Cost-Sensitive Robustness against Adversarial Examples. *International Conference on Learning Representations (ICLR)*, 2019.